How to cite: *Angew. Chem. Int. Ed.* **2022,** *61,* e202205931
International Edition: doi.org/10.1002/anie.202205931
German Edition: doi.org/10.1002/ange.202205931

Polymerization Hot Paper

One-For-All Polyolefin Functionalization: Active Ester as Gateway to Combine Insertion Polymerization with ROP, NMP, and RAFT

Huong Dau, Enkhjargal Tsogtgerel, Krzysztof Matyjaszewski, and Eva Harth**

Abstract: This work develops the Polyolefin Active-Ester Exchange (PACE) process to afford well-defined polyolefin–polyvinyl block copolymers. α-Diimine Pd^{II}-catalyzed olefin polymerizations were investigated through in-depth kinetic studies in comparison to an analog to establish the critical design that facilitates catalyst activation. Simple transformations lead to a diversity of functional groups forming polyolefin macro-initiators or macro-mediators for various subsequent controlled polymerization techniques. Preparation of block copolymers with different architectures, molecular weights, and compositions was demonstrated with ring-opening polymerization (ROP), nitroxide-mediated polymerization (NMP), and photoiniferter reversible addition–fragmentation chain transfer (PI-RAFT). The significant difference in the properties of polyolefin–polyacrylamide block copolymers was harnessed to carry out polymerization-induced self-assembly (PISA) and study the nanostructure behaviors.

Introduction

In the search for functionalized polyolefins with enhanced surface properties, block copolymers comprising polyolefins and polar polymers stand out as one of the most desirable materials.[1] This is due to their ability to embody a substantial amount of functionalities while conserving the advantageous thermal and mechanical features of their constituent homopolymers. While a variety of olefinic block copolymers have been readily accessible via the advancement in metal-catalyzed living polymerization, synthetic platforms for polyolefin–polar block copolymers remain scarce due to the tremendous difference in reactivity between the two monomer classes.[2] The major drawbacks of the traditional method relying on anionic polymerization involves multiple stepwise syntheses, stringent experimental conditions, and limited monomer types.[3] The development of late transition metal catalysts has greatly facilitated the exploration of functionalized polyolefins owing to their functional group tolerance. However, the polymers generated via the sole coordination–insertion technique are limited to random architectures.[1a,4] Hence, end-functionalized polyolefins attained via post-polymerization remain the dominant approach for the preparation of polyolefin–polar block copolymers by combined polymerization techniques.[3b,5]

One of the applied approaches is catalytic chain transfer polymerization (CCTP), which offers a pathway to introduce functional groups derived from the chain transfer agents (CTA). Mecking et al. reported a catalytic chain transfer polymerization of ethylene using α-diimine Pd^{II} catalysts and TIPNO-functionalized silanes as the CTAs.[6] Subsequent chain extensions with styrene or *n*-butyl acrylate via nitroxide mediated polymerization (NMP) yielded diblock copolymers. While the study successfully bridged insertion and controlled radical polymerization, the limitations include a laborious synthesis for the alkoxyamine-CTA, as well as the excess amount of CTAs (100 equivalents) needed for a sufficiently high degree of functionalization (80 %). Additionally, high CTA loading resulted in the high dispersity and loss of livingness during insertion polymerization. More recently, we reported the Metal–organic Insertion Light initiated Radical (MILRad) functionalization, a strategy that allows the transformation of insertion polymerization to controlled radical polymerization under mild conditions and a light-assisted process.[7] This technique relies on the susceptibility of the Pd-alkyl bond to homolytic cleavage under blue light irradiation.[8] Thus, the growing polyolefin chains can be captured by radical/spin trapping agents to produce corresponding macroinitiators that are capable of chain extension with styrene, isoprene, and acrylic monomers to produce di- and tri-block copolymers. However, the polar functionalities of nitroxide trapping agents promoted chain transfer side reactions during the light cycle and resulted in the formation of unfunctionalized PE at a ratio of 20–50 % in the polyolefin precursors. The limitations of these aforementioned strategies emphasize the need for an alternative synthetic protocol that accomplishes functionalized polyolefins with high uniformity in quantitative yields with targetable molecular weights.

Functionalized catalysts that are capable of polymerizing ethylene in a living manner require selective introduction of functional groups at the polymer chain ends. Previous work by Ye et al. demonstrated the preparation of diblock copolymers containing PE and PS/P(*n*-BA) through tandem

[*] H. Dau, E. Tsogtgerel, Prof. Dr. E. Harth
Department of Chemistry, Center of Excellence in Polymer Chemistry, University of Houston
3585 Cullen Boulevard, Houston, TX 77030 (USA)
E-mail: harth@uh.edu
Prof. Dr. K. Matyjaszewski
Department of Chemistry, Carnegie Mellon University
4400 Fifth Avenue, Pittsburgh, PA 15213 (USA)
E-mail: km3b@andrew.cmu

coordination–insertion polymerization (CIP) and ATRP.[9] The synthesis employed a Brookhart's type palladium diimine chelate functionalized with a 2-bromoisobutyryl end-group that can polymerize ethylene in a living fashion. However, the catalyst productivity remains low (TOF = 154/h), and a discrepancy in molecular weight calculated by GPC analysis and gravimetrically method was observed, which was attributed to an incomplete catalyst activation. In previous work, we reported a binuclear cationic Pd-diimine complex bearing an octafluoro diacrylate linker that can polymerize ethylene in a living manner with higher TOF compared to its analogs.[8a] The higher productivity was attributed to the strong electron-withdrawing ability of the fluorine linker, which leads to faster initiation. In the same study, to confirm the PMA-PE-PMA triblock architecture of the polymer obtained from the aforementioned catalyst via MILRad polymerization, we carried out a hydrolysis experiment using 1,8-diazabicyclo[5.4.0]undec-7-ene (DBU), a non-nucleophilic base. This discovery inspired us to develop a strategy called Polyolefin Active-Ester Exchange (PACE) to install an active ester unit on the terminal polyolefin, which was derived from a pre-functionalized catalyst (Figure 1). To achieve complete functionalization, the catalyst must polymerize ethylene/α-olefins in a living manner. Additionally, the active ester handle can be quantitatively transformed into functional groups that give access to controlled polymerization methods. We hypothesized that when these two requirements are met, various block copolymers can be prepared.

Herein, we report a pentafluorophenyl ester (PFPh) chelated palladium catalyst that allows for the preparation of single-site functionalized polyolefins. We envisioned that the lability of the PFPh terminal unit would facilitate the "on-demand" transformation to obtain polyolefin macrointiators that can be chain extended via different polymerization techniques. The effects of functional groups on the catalyst activity toward ethylene and α-olefins polymerization were investigated through comparative kinetic studies with a methyl acrylate chelated analog. Following the polyolefin functionalization, facile post-polymerization through aminolysis and transesterification affords polyolefin macroinitiators for subsequent living/controlled polymerization techniques including ring-opening polymerization (ROP), nitroxide-mediated polymerization (NMP), and photoiniferter reversible addition–fragmentation chain transfer (PI-RAFT), yielding low dispersity polyolefin–polyester and polyolefin–polystyrene diblock copolymers (Figure 1). As the livingness was maintained during both polymerization methods, this technique potentially serves as a versatile platform for the preparation of novel polyolefin-containing block copolymers with a high degree of flexibility in molecular weight and composition.

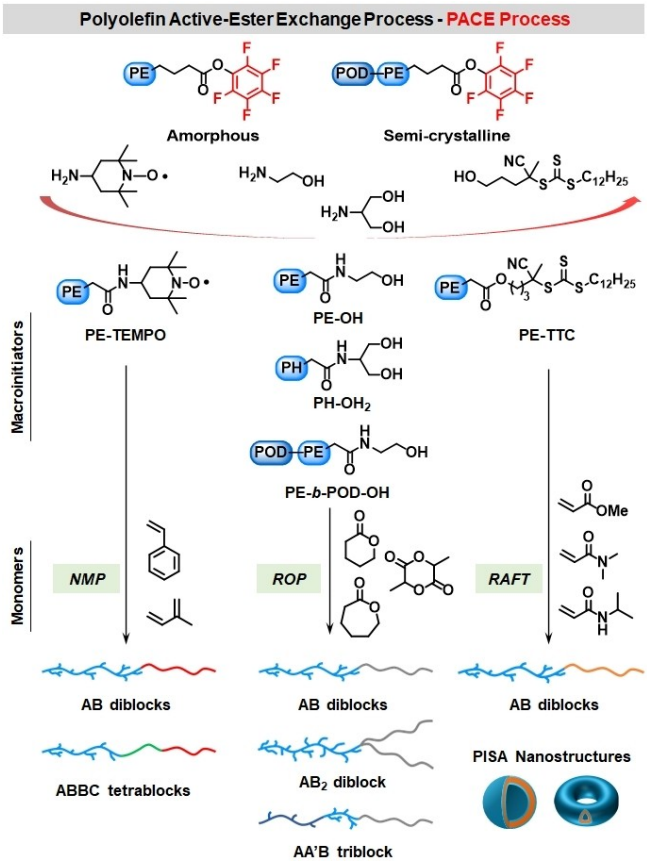

Figure 1. Overview of PACE process allowing the combination of CIP with ROP, NMP, and RAFT for the synthesis of well-defined hybrid polymers.

Results and Discussion

The active ester functionalized palladium(II) diimine catalyst was prepared by a single insertion of pentafluorophenyl acrylate to the Pd–alkyl bond of the precursor using an adapted procedure (Supporting Information Section 2.3).[10] NMR analyses of the products revealed the predominant formation of a six-membered ring chelate via 2,1-insertion with approximately 90 % regioselectivity. 1,2-insertion also occurred, resulting in the generation of a five-membered chelate (10 %). This result is in agreement with previously reported studies by Brookhart and co-workers.[10,11] ^{19}F NMR experiments were performed to confirm the attachment of the fluorinated ester. Additionally, the structure of the major isomer was verified by X-ray diffraction analysis after recrystallization by slow diffusion of pentane into a solution of **1** in CH_2Cl_2 at −20 °C (Figure 2).

Ethylene polymerization was carried out at typical controlled conditions (5 °C, 400 psi) to investigate the performance of catalyst **1** (Figure 3B). The polymerization livingness was evidenced through low dispersities that remained during the reaction, in addition to the linear increase of molecular weight versus time. Due to the chelate structure, ethylene polymerization catalyzed by **1** can directly generate semi-telechelic polyethylene bearing a pentafluoro ester moiety (PE-PFPh) that was introduced by the initiating species at the beginning of the propagation. GPC analysis with dual detection showed a good overlap of RI and UV traces, which was detectable because of the

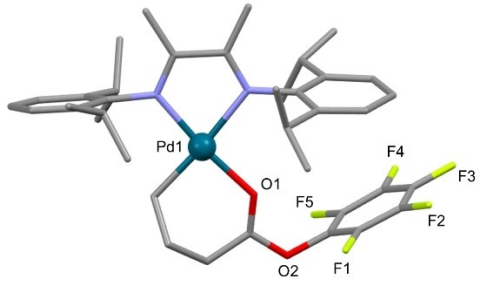

Figure 2. X-ray structure of major isomer found in complex **1**.[12] Hydrogen atoms and the BArF counterion are omitted for clarity.

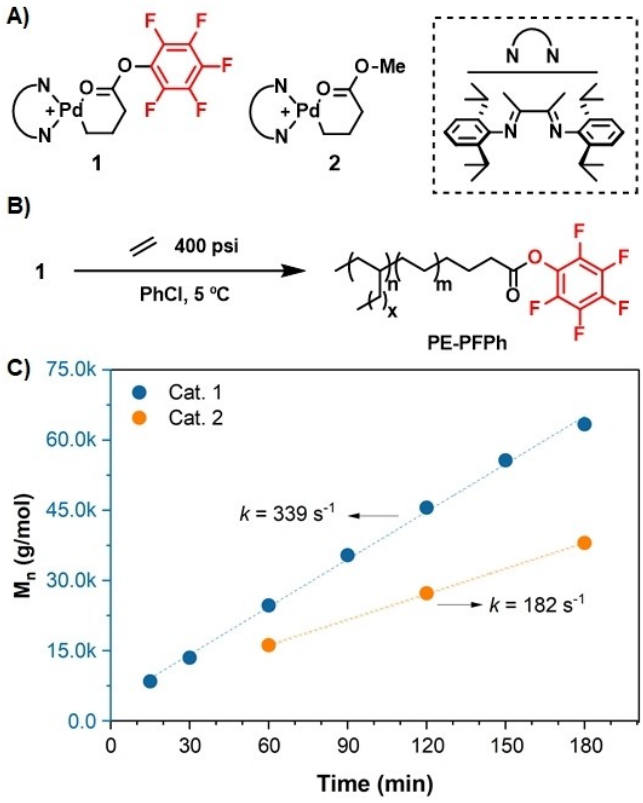

Figure 3. A) Pentafluoro-functionalized palladium diimine catalyst and its methyl acrylate analog. B) Synthesis of PE-PFPh. C) Comparison of ethylene polymerization rate using cat. **1** versus cat. **2**.

aromatic polymer end-group. ^{1}H NMR analysis of the PE-PFPh showed a distinctive peak of CH_2COOPFPh at 2.66 ppm, suggesting a deshielding effect caused by the terminal fluorinated group. This was further confirmed through observed ^{19}F NMR resonances that are similar to the reported values of a small molecule model.[13] A good correlation between molecular weight determined by GPC ($M_n^{15\,min}$ = 8600) and ^{1}H NMR chain-end analysis ($M_n^{15\,min}$ = 7700), as well as the lack of olefinic resonances indicated the high chain-end fidelity of the polymerization.

In order to gain more insights into the effect of ester substituents on catalyst activity, a methyl acrylate chelated Pd diimine, complex **2**, was also synthesized (Figure 3A). Similar to previous studies, the synthesized catalyst comprises a mixture of six- and five-membered chelate isomers with a ratio of 83 % and 17 %. Under similar conditions, the rate of ethylene polymerization when using **2** is slower, compared to catalyst **1**. This can be explained by the slow initiation process due to the unfavorable equilibrium between the stable six-membered ring chelate and the Pd-ethylene complex which is required for further propagation.[10,11] Another feature that is regularly found in Pd-chelate catalyzed ethylene or α-olefins polymerization is the discrepancy between the molecular weight by GPC and catalyst productivity that is based on the weight of polymers obtained per mole of catalyst.[9,14] For example, Brookhart and co-workers pointed out that when employing cat. **2**, the M_n calculated based on TOF was 2.5 times lower than determined by GPC, which was attributed to the significant overestimation of polystyrene standards.[14] However, we speculated that the substantially low M_n^{TOF} was caused by poor activation of catalyst **2**, which resulted in an apparently low molar ratio of [ethylene consumed]:[Pd]. ^{1}H NMR of crude aliquots collected at different time points showed incomplete activation of catalyst **2**. Specifically, by utilizing the integration of the methoxy region of catalyst **2**, compared to the resultant PE, the catalyst activation is estimated to be 13 % after 15 minutes of polymerization, then increased to ca. 39 % after 1 hour. The low catalyst activation explains the significant difference between M_n^{GPC} (16300) and M_n^{TOF} (6800) in ethylene polymerization using **1** after one hour (Table S3). On the other hand, owing to the destabilization of the carbonyl coordination caused by the strong electron-withdrawing group, quantitative catalyst activation was achieved with **1**, leading to a fast initiation process. This was evident by the observed three times higher productivity of **1** (TOF = 777/h) compared to **2** (244/h), as well as the good correlation between molecular weight estimated by GPC and TOF under similar reaction conditions (Table S3).

Chelate opening with α-olefins is considered to be more challenging compared to ethylene because of steric hindrance.[15] As a consequence, α-olefin polymerization employing **2** was previously reported to be performed at low temperature (0 °C) to slow down the propagation process regarding initiation to eventually obtain better controlled polymerization. With the insights gained from ethylene polymerization studies, we hypothesized that **1** can polymerize 1-hexene at room temperature in a living fashion thanks to fast initiation. As the resonances of the PFPh group during chain growth are different in comparison to when bound to Pd, in situ ^{19}F was employed to address the initiation efficiency. In detail, to an NMR tube containing a solution of 1 in chloroform-*d*, 1-hexene monomers (100 equiv) were added and the reaction was immediately submitted to ^{19}F NMR spectroscopy measurements. A complete initiation was confirmed by the clean-upfield shift observed in the spectrum (Figure S11). Surprisingly, the resultant polyhexene by **1** (PH-PFPh) exhibited a different microstructure from previously reported data.[16] The degree of branching of PH-PFPh was calculated to have 149 branches (B) per 1000 carbons (C), while polyhexene

derived by **2** showed 95B/1000 C. Quantitative ^{13}C NMR analysis shows a good agreement with ^{1}H NMR data (144B/1000 C), with significant enchainment of longer branches (C2–C4 branches) compared to regular poly(1-hexene) (Figure S13).[8a,16] To gain a deeper understanding of 1-hexene polymerization via this system, kinetic studies were performed assisted by NMR and GPC analyses. Tracking monomer conversion via ^{1}H NMR revealed that polymerization and isomerization is occurring simultaneously. Isomerization of 1-hexene to 2- and 3-hexene proceeded rapidly and was completed after 30 minutes of the reaction. Then, the polymerization slowed down as the binding affinity and insertion rate of internal hexenes were less than for 1-hexene due to steric effects.[16] This concurrent isomerization-polymerization resulted in two distinctive linear kinetic profiles (time vs. monomer conversion and conversion vs. molecular weight) of living polymerization, which were separated by the time point where quantitative isomerization was achieved (Figure 4A). This phenomenon resulted in the formation of an olefin block copolymer with different branching structures (Figure 4B). After 2.5 hours of the reaction, highly branched polyhexene was obtained with $M_n = 43\,100$ (85 % conversion), and narrow molecular weight distribution ($Đ = 1.1$) (Table S4). As the livingness in traditional Pd-diimine catalyzed olefin polymerization is commonly only conceded with a linear increase in molecular weight versus time, this finding represents a different facet when addressing the livingness in the isomerization-polymerization system.[16,17] On the contrary, the polymerization

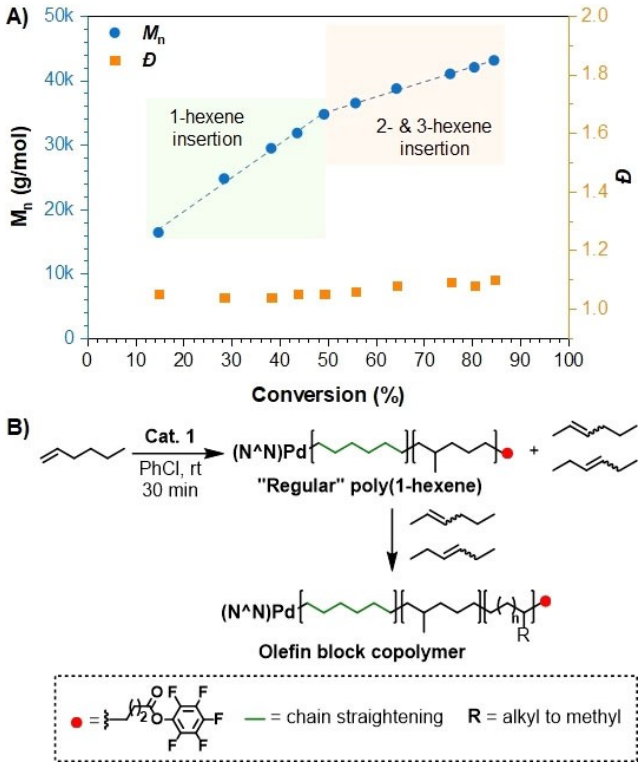

Figure 4. A) Kinetic profile of cat. **1**-catalyzed isomerization polymerization. B) Mechanism of highly branched PH derived from cat. **1**.

with catalyst **2** is drastically slower, affording only 24 % conversion and 12 % of catalyst activation after 4 hours forming polymer with higher dispersity ($Đ = 1.32$) (Table S5).

Similarly, isomerization to mostly 2-hexene was observed, but continuously increased throughout the reaction, suggesting a modest insertion of internal hexenes occurred. Furthermore, the microstructure of polyhexene derived from the two catalysts are significantly different. Typical 1-hexene polymerization with a chain walking catalyst proceeds through a chain straightening mechanism, in which the terminal alkenes can insert into the Pd–C bond via 1,2- or 2,1-insertion followed by complete chain walking to the primary Pd-alkyl bond prior to the next insertion.[15,16] This afforded polyhexene with linear methylene sequences and a majority of methyl branches on the polymer backbone. In contrast, insertions of internal hexenes cannot generate linear segments. As a consequence, polyhexene produced with **1** displayed thermal characteristics of highly amorphous materials with $T_g = -70\,°C$, significantly lower compared to regular poly(1-hexene) with $T_g = -44\,°C$ and $T_m = 0\,°C$.

As the integrity of living ethylene/α-olefins polymerization using cat. **1** is established, we sought to manipulate the crystallinity of the resultant polyolefins by using 1-octadecene, a long-chain α-olefin. This led to the introduction of linear segments (C16–18) as an outcome of the "chain straightening" fashion.[16–18] Polymerization via sequential addition of ethylene and 1-octadecene using **1** as catalyst afforded polyethylene-polyoctadecene diblock copolymers (PE-*b*-POD) with semicrystalline properties (42B/1000C, $T_m = 76.5\,°C$, $87.9\,°C$). ^{1}H NMR analysis indicated that the PFPh end-group remained and no chain transfer side reactions occurred (Figure S18A). The livingness of the block polymerization was also evident by a clean shift to a higher molecular weight region (Figure S18B).

With the PFPh-functionalized polyolefins in hand, one-step end-group transformations were performed to attain corresponding macroinitiators that are capable of undergoing controlled polymerization including ROP and reversible-deactivation radical polymerization such as NMP or RAFT. In order to showcase the versatility of this method, we utilized commercially available exchange agents in aminolysis/transesterification with PO-PFPh that can be performed under mild reaction conditions owning to the high lability of the PFPh terminal group. 2-Aminoethyl alcohol (ethanolamine) and 2-amino-1,3-propanediol (serinol) were picked to introduce hydroxy end-groups to polyolefin precursors. 4-Amino-2,2,6,6-tetramethylpiperidine-1-oxyl (4-Amino-TEMPO) stable radical was selected to produce a macroradical that can serve as a mediating agent in NMP but also for the potential of undergoing radical coupling reaction for block copolymer synthesis.[19] Finally, as coordination-insertion/RAFT combined examples remain scarce, transesterification with 4-cyano-4-[(dodecylsulfanylthiocarbonyl)sulfanyl]pentanol (CDP), a trithiocarbonate (TTC) chain transfer agent, was also performed to obtain a PE-based macroRAFT agent.[1a] Additionally, polymerization of a broad range of monomers

including cyclic esters, styrene, dienes, acrylamides, and acrylates were explored.

The aminolysis of PE-PFPh was first carried out with ethanolamine to yield a hydroxy-terminated polyethylene (PE-OH, $M_n = 5900$, $Đ = 1.02$). ^{1}H NMR analysis of the resultant polymer showed the disappearance of the 2.65 ppm signal indicative of the CH_2 proton at the α-position with respect to the pentafluoro ester group (ca. 2.65 ppm), which shifted to 2.21 ppm when attached to the amide moiety. Additionally, the integration matched the –CH_2–CH_2– protons found in the attached ethanolamine, which indicates quantitative transformation to PE-OH (Figure S19).

Typical conditions of DPP-catalyzed ROP of δ-valerolactone (δ-VL) and ε-caprolactone (ε-CL) were employed using PE-OH to yield polyethylene-polyester diblock copolymers.[20] Full consumption of the PE-OH macroinitiator was revealed through ^{1}H NMR spectroscopy of the isolated products as the hydroxymethyl (ca. 3.72 ppm) no longer appeared, coupled with a new signal at 3.65–3.67 ppm, corresponding to the hydroxymethyl of the polyester end-group (Figure S19, S26, S27). Furthermore, GPC traces also validate the efficient initiation as a complete shift to a higher molecular weight region while maintaining low dispersities were seen (Table 1,, entries 1, 2, Figure 5A and Figure S31A). A chain extension of PE-*b*-PVL (Table 1, Entry 1) with ε-CL was then carried out to assess the chain-end fidelity of the block copolymer. An expected shift of the diblock to the final triblock copolymer of PE-*b*-PVL-*b*-PCL with narrow molecular weight distribution ($M_n = 15200$, $Đ = 1.10$) was observed, highlighting the livingness of the diblock precursor (Figure 5A). Similarly, PE-*b*-POD bearing an OH end-group (PE-POD-OH, $M_n = 19600$, $Đ = 1.16$) was prepared and employed for organocatalyzed ROP with *rac*-lactide and δ-VL. This polyolefin diblock macroinitiator gave a triblock copolymer comprising a new polylactide (PLA) segment that reached a molar mass of 29.7 kDa with a unimodal distribution ($Đ = 1.16$) (Figure 5B).

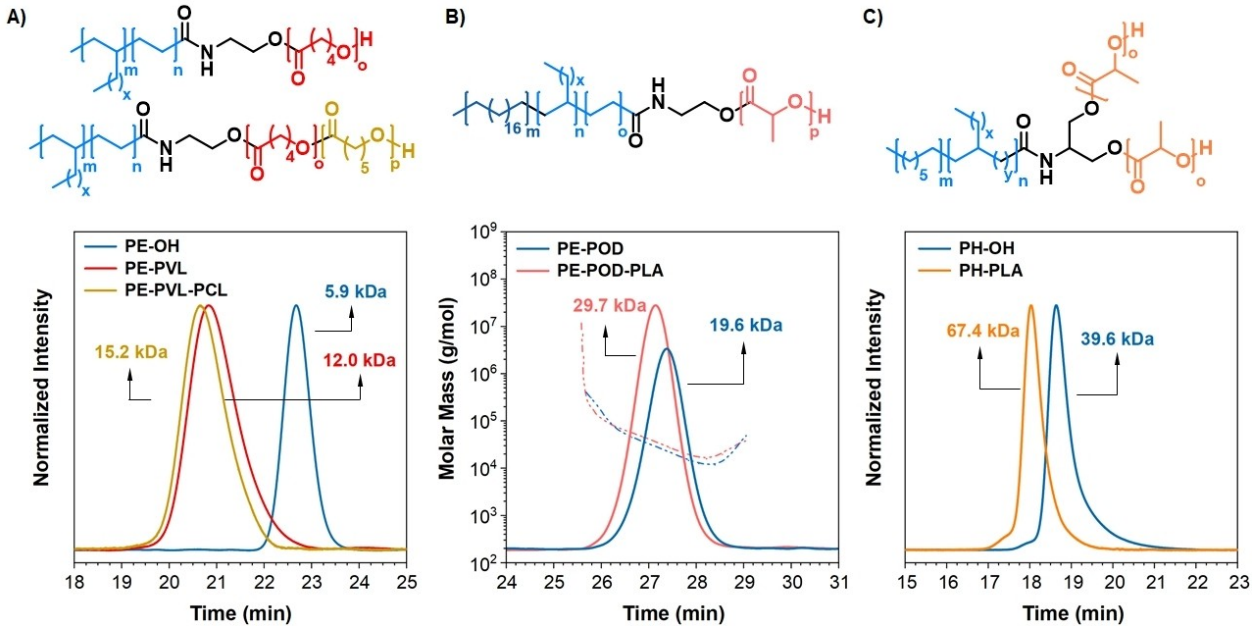

Figure 5. GPC traces of di-, tri-, and "star-like"-block copolymers synthesized via ROP of various cyclic esters initiated by hydroxy functionalized polyolefins.

Table 1: Selected polyolefin–polyester block copolymers.

Entry	Sample	Macroinitiator	Polyolefin Block M_n	Polyolefin Block $Đ$	Co-monomers	Polyolefin-*b*-polyester M_n	Polyolefin-*b*-polyester $Đ$	T_g [°C]	T_m [°C]
1[a,c]	PE-PVL	PE-OH	5900	1.02	δ-VL	12000	1.10	−64.0	50
2[a,c]	PE-PCL	PE-OH	5900	1.02	ε-CL	14000	1.05	−64	54
3[a,c]	PE-PVL-PCL	PE-PVL	12000	1.10	ε-CL	15200	1.10	ND	ND
4[a,d]	PE-POD-PVL	PE-POD-OH	19600	1.16	δ-VL	21800	1.16	ND	ND
5[a,d]	PE-POD-PVL	PE-POD-OH	19600	1.16	δ-VL	32400	1.11	−64	53, 72, 85
6[b,d]	PE-POD-PLA	PE-POD-OH	19600	1.16	*rac*-LA	29700	1.16	52	71, 85
7[b,c]	PH-PLA$_2$	PH-OH$_2$	39600	1.12	*rac* -LA	67400	1.05	−48/48	–

[a] Catalyst used for ROP: **DPP**. [b] Catalyst used for ROP: **MTBD**. [c] Molecular weight and dispersity index ($Đ$) were determined by GPC analysis with samples run in THF at 40 °C calibrated to polystyrene standards. [d] Molecular weight and polydispersity index ($Đ$) were determined by GPC analysis with samples run in TCB at 150 °C calibrated to polystyrene standards.

In the case of chain extension with δ-VL, interestingly, triple detection HT-GPC showed that the elution of the obtained triblock copolymers shifted backward as well as a decrease in refractive index (RI) intensity as the PVL incorporation increased (Figure S31B). This phenomenon can be explained by the hydrodynamic volume of the resulting PE-*b*-POD-*b*-PVL being smaller than the polyolefin precursor in the eluent solvent (trichlorobenzene).

Despite this, the dispersity of the generated triblock copolymers slightly decreased (1.16 to 1.11) as molecular weight increased (Table 1, entry 5), highlighting the uniformity and livingness of the polymerization. In addition to ethanolamine, serinol was selected to react with the end-product of the hexene kinetic study (Section 3.3) to achieve a dual-hydroxy functionalized polyhexene (PH–OH_2). A successive extension was demonstrated with *rac*-lactide using MTBD as a catalyst, which afforded a "star-like" triblock architecture of PH-PLA_2 with $M_n = 67\,400$ and lower dispersity ($Đ = 1.05$) compared to its macroinitiator (Table 1, entry 6, and Figure 5C).

PE bearing a nitroxide stable radical represents an opportunity for the formation of polyolefin–polyvinyl block copolymers via the NMP technique. This concept was first introduced by our group via the MILRad spin-trapping functionalization, which can be used to produce PE-*b*-PS block copolymers.[7,8] However, the crude product of functionalization needs to go under dimethyl sulfide or acetonitrile treatment to release all of the macroradicals. Additionally, due to the polar functionalities of the spin trapping agent, chain transfer side products were formed, entailing homoPE removal after NMP to attain pure block copolymers.

This work strives to overcome this limitation by quantitatively introducing a TEMPO radical unit at the chain end of PE. Aminolyses of PE-PFPh precursors with 4-amino-TEMPO afford PE-TEMPO macroradicals, which was characterized by a combination of electron paramagnetic resonance (EPR), NMR, and GPC (Figures S21, S22).

EPR resonances of isolated PE-TEMPO macroradicals displayed a triplet with hyperfine coupling constants of $a_N = 15.46$ G and are consistent with the literature value of TEMPO (Figure 6B).[21] PE-TEMPO ($M_n = 7800$, $Đ = 1.04$; Table 2) was then used as the macro-mediating agent in NMP polymerization with styrene using benzoyl peroxide (BPO) as a radical initiator in an adapted procedure.[22]

To avoid self-initiated free radical polymerization of styrene at high temperature, a mixture of PE-TEMPO, BPO, and styrene in toluene was first heated to 85 °C (4 hours) to generate the alkoxyamine adduct in situ. Next, the reaction temperature was subsequently raised to 120 °C to promote chain propagation (Figure 6A). Regular sampling of the reaction mixture revealed a long induction period as no significant shift in GPC elution was recorded after 7.5 hours. However, as the polymerization progressed, well-defined PE-*b*-PS were obtained with narrow molecular weight distribution ($M_n = 10\,300$–$22\,600$, $Đ = 1.04$–1.12) (Figure 6C). This method was also used to prepare PE-*b*-PS with a different composition ($M_n = 47\,500$, $Đ = 1.12$) with a higher PE block length by utilizing PE-TEMPO with a molecular weight of 27 700 ($Đ = 1.02$) as the macroinitiator. The long induction period was attributed to the built-up free nitroxide

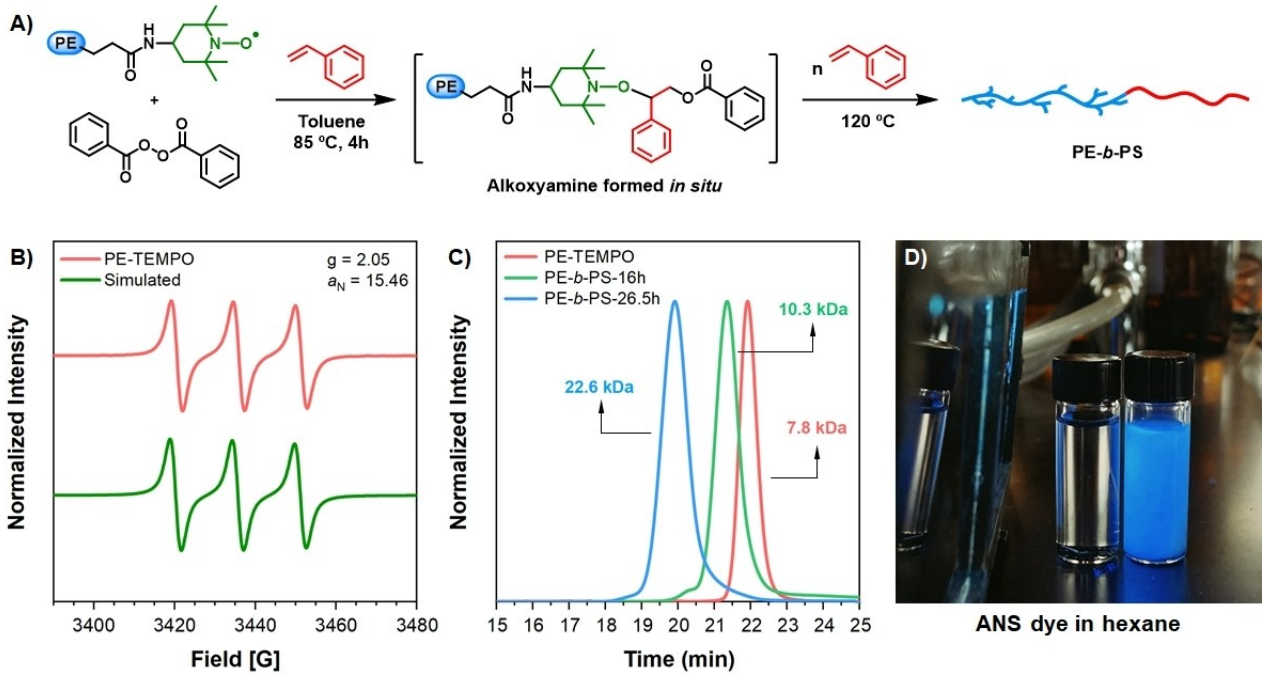

Figure 6. A) Synthesis of PE-b-PS using PE-TEMPO as a macromediator. B) CW X-band (9.5 MHz, rt) EPR spectra of PE-TEMPO and simulated signals of TEMPO radical. C) GPC traces of PE-*b*-PS diblock copolymers at different time points during chain extension with styrene via NMP. D) Encapsulation of ANS fluorescent dye with PE-*b*-PS in hexanes.

Table 2: Selected polyolefin–polyvinyl block copolymers.

Entry	Sample	Macroinitiator	Polyolefin Block M_n	$Đ$	Co-monomers	Polyolefin-*b*-polyvinyl M_n	$Đ$	T_g [°C]	T_m [°C]
1[a,c]	PE-PS	PE-TEMPO	7800	1.04	Styrene	22600	1.12	ND	ND
2[a,b,c]	PE-PS	PE-TEMPO	7800	1.04	Styrene	15300	1.19	ND	ND
3[a,c]	PE-PS	PE-TEMPO	27700	1.02	Styrene	47500	1.07	ND	ND
4[c]	PE-PS-PS	PE-PS	47500	1.12	Styrene	60000	1.32	−67, 100	–
5[c]	PE-PS-PS-PI	PE-PS-PS	60000	1.32	Isoprene	72000	1.29	−62, 104	–

[a] BPO was used as an initiator. [b] CSA (0.036 M) was added for rate acceleration. [c] Molecular weight and dispersity index ($Đ$) were determined by GPC analysis with samples run in THF at 40 °C calibrated to polystyrene standards.

throughout polymerization as a consequence of termination.[23] To tackle this issue, camphorsulfonic acid (CSA, 0.036 M) was added to the reaction, which served as a scavenger for free nitroxides and accelerated chain propagation.[24] This afforded PE-*b*-PS with $M_n = 15300$ after only 6 hours of polymerization (Figure S34C).

The chain-end fidelity of the PE-*b*-PS diblock copolymers was apprised through continuous chain extension with styrene and isoprene. Particularly, the PE-*b*-PS ($M_n = 47500$, $Đ = 1.12$) was used as a macroinitiator for the radical polymerization of styrene at 120 °C. The induction period no longer occurred and ABB-type PE-*b*-PS-*b*-PS triblock copolymer with high molecular weight ($M_n = 60000$) and reasonable dispersity ($Đ = 1.32$) were obtained. The isolated product was further extended with isoprene to give an ABBC tetrablock architecture of PE-*b*-PS-*b*-PS-*b*-PI ($M_n = 72000$, $Đ = 1.29$). ^{1}H diffusion-ordered NMR spectroscopy (DOSY) was performed on the PE-*b*-PS diblock copolymers (Table 2, entry 3, Figure S44). The 2D spectrum of the block copolymer exhibited a single resonance whereas the singles of the PE segment (0.8–1.22 ppm) and PS segment (6.42–7.09 ppm) were aligned tightly around the same diffusion coefficient (4.05×10^{-11} cm^2 s^{-1}), confirming a blocky architecture. The selective solubility of this hybrid material allows the preparation of micelle-size dispersion via a self-assembly mechanism. Specifically, the PE-*b*-PS (Table 2, entry 1) could be dispersed in hexanes (selective solvent for PE) and encapsulate 8-anilino-naphthalene sulfonic acid (ANS dye), an environmentally sensitive fluorescent probe. The dispersion of the block copolymer with this probe exhibits fluorescent properties upon UV light irradiation (Figure 6D, right), whereas in the control experiment, no fluorescence was observed (Figure 6D, left).

Despite its excellent reactivity towards aminolysis, the pentafluorophenyl ester group is not prone to transesterification because of the backward reaction demonstrated in earlier reports.[13b] Higher conversion (up to 90 %) could be achieved when using TBD as the catalyst.[13a] However, the instability of RAFT agents towards aminolysis precludes the use of this organocatalyst for the current study.[25] Attempts were carried out by employing DBU and MTBD for transesterification with the CDP, however, the conversions remained low (less than 50 % after 24 hours). Eventually, an adapted procedure based on a recent study by Theato and co-workers was employed to accomplish a near quantitative conversion.[13c] Specifically, transesterification of PE-PFPh with CDP was performed using a milder DMAP/DMF base system and toluene as the solvent at 85 °C. In the NMR spectrum of the isolated product, a new triplet corresponding to the α-hydrogens of the ester moiety (–C$\boldsymbol{H}_2$CO, $\delta =$ 4.12 ppm) was observed. The integration of this peak matched with that of S–C$\boldsymbol{H}_2$ (3.32 ppm) on the RAFT-Z group, which suggested the preservation of the RAFT agent under this condition (Figure S23, S24). The complete disappearance of the C$\boldsymbol{H}_2$CO$_2$PFPh indicates the quantitative conversion of the parental PE. Additionally, GPC traces of the PE-TTC showed a stronger absorption by UV detection compared to the PE-PFPh precursor (Figure S25A). UV/Vis spectroscopy of the PE-TTC also exhibits two absorption bands corresponding to $\pi \rightarrow \pi^*$ transition (ca. 310 nm) and $n \rightarrow \pi^*$ (ca. 450 nm), resembling closely the CDP's spectroscopy. We sought to explore the ability of PE-TTC in PI-RAFT polymerization to initiate acrylamide monomers by exciting the macroRAFT PE using UV light irradiation (365 nm). In a typical reaction, PE-TTC (25 mg mL^{-1}, $M_n = 16000$, $Đ = 1.02$) and the acrylamide monomers (620 eq) were dissolved in toluene, followed by degassing via three consecutive freeze-pump-thaw cycles. The reaction vial was then sealed under nitrogen and placed in a photoreactor (PhotoCube) and UV light was turned on to start the polymerization (Supporting Information, Section 5.3). The polymeric material collected after the polymerization was difficult to purify using conventional methods such as precipitation. Particularly, in the case of the chain extension of PE-TTC with DMA, the material formed a cloudy dispersion in both methanol and hexane, which was attributed to the ability to self-assemble into nano-objects in a selective solvent for their homopolymer constituent. The dispersion of PE-*b*-PDMA in methanol was analyzed by transmission electron microscopy (TEM), revealing the formation of micellar structures with an average diameter of 172 nm (Figure S49). DOSY spectra of the isolated polymer also pointed towards the formation of the blocky structure, as the signals corresponding to PE (0.8–1.22 ppm) and PDMA (2.87–3.10 ppm) exhibit a similar diffusion coefficient (Figure 7A). It is noteworthy that the molecular weight arising from GPC analysis equipped with the RI detector of the block copolymers would not accurately correlate to their true molecular weights as a consequence of changes in hydrodynamic volume. Particularly, the highly branched PE described in the study is commonly characterized using THF as eluent, whereas the eluent for polyacrylamides is typically

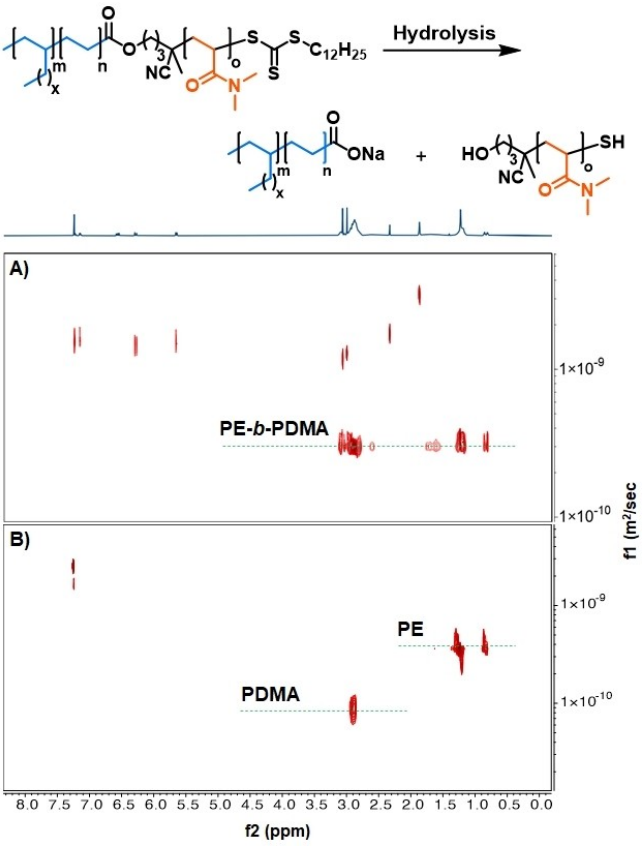

Figure 7. A) ^{1}H DOSY NMR (600 MHz, chloroform-*d*, 298 K): A) PE-*b*-PDMA diblock copolymers; B) a mixture of PE and PDMA homopolymers after hydrolysis of the parental diblock.

DMF with added LiBr to avoid dipole interaction.[26] Although the obtained polymers are soluble in various solvents, attempts to characterize the sample molecular weight in THF, chloroform, and DMF/LiBr gave different results. Due to this inconsistency, hydrolysis of the ester linkage was carried out to obtain a mixture of homopolymers that can be analyzed in their suitable solvents to obtain reliable data. DOSY experiments were implemented to confirm the successful cleavage of the block copolymers, as shown in Figure 7B, where two distinct diffusion coefficients correlated to the PE and PDMA homopolymers were recorded. The hydrolyzed product was then prepared in THF or DMF/LiBr separately and subjected to GPC analyses with the corresponding eluents.

As expected, the THF-GPC trace of the hydrolyzed polymer overlapped well with its PE-TTC precursor, and the DMF-GPC showed a unimodal trace of PDMA with a molecular weight of 57700 and $Đ = 1.4$ (Figure S39).

These results motivated us to explore PE-TTC-mediated polymerization-induced self-assembly (PISA) with *N*-isopropylacrylamide (NIPAM) due to its solvophobic interaction with toluene (Table 3; Figure 8A).[27] The initial transparent reaction medium was turbid after 6 hours of polymerization with 82 % of monomer conversion.

The DOSY spectrum of the isolated polymer showed a single coefficient diffusion, indicating the generation of PE-*b*-PNIPAM diblock copolymer. Hydrolysis of the diblock copolymer was again conducted to obtain the molecular weight of the polyacrylamide segment. DMF GPC analysis indicated a unimodal with $M_n = 90800$, with a relatively broad molecular weight distribution ($Đ = 1.7$).

We attributed the observed high dispersity to the degradation of the TTC end-group under UV light at high conversion (82 %) as previously suggested.[28] To probe the PISA result, an aliquot of the crude reaction was diluted with toluene and analyzed with dynamic light scattering (DLS) and TEM. DLS data suggested the formation of nanostructured objects with an average diameter of 190 nm. One of the major advantages of PISA is its ability to provide access to higher-order morphology. In the presented case, TEM imaging revealed the generation of vesicles and donut-like structures (Figure 8B).

Considering the water-soluble and thermo-responsive features of PNIPAM, we anticipated that the introduction of the PNIPAM segment would grant these appealing properties to the PE-*b*-PNIPAM diblock copolymers. The PE-*b*-PNIPAM can be readily prepared in water at 0.5 w% concentration by sonication at the ambient temperature, resulting in a transparent dispersion. The hydrodynamic volume as a function of temperature was monitored through DLS measurements per 2 °C interval. The particle sizes were approximately 80 nm within the range of 20–34 °C, then increased rapidly, reaching ca. 320 nm at 45 °C (Figure 8C). This suggested the coil-to-globule transition and the formation of large aggregates due to hydrophobic interactions between PNIPAM chains.[29] To the best of our knowledge, this study represents the first synthetic example of a diblock copolymer comprising PE and polyacrylamide (PA) as well as PISA involving PE and PNIPAM.

Due to the high dispersity observed in the PE-*b*-PA, we also performed chain extension employing PE-TTC ($M_n =$

Table 3: Selected polyolefin–polyacrylamide/acrylate block copolymers.

Entry	Sample	Polyolefin Block[a]			Co-monomers	Polyolefin-*b*-polyvinyl		T_g [°C]	T_m [°C]
		Macroinitiator[a]	M_n	$Đ$		M_n	$Đ$		
1	PE-PDMA	PE-TTC	16000	1.02	DMA	73700[b]	–	−67/108	–
2	PE-PNIPAM	PE-TTC	16000	1.02	NIPAM	106800[b]	–	−67/130	–
3	PE-PMA	PE-TTC	14500	1.01	MA	35300[a]	1.12	−67/13	–

[a] Molecular weight and dispersity index ($Đ$) were determined by GPC analysis with samples run in THF at 40 °C calibrated to polystyrene standards. [b] Molecular weight was calculated by the addition of the molecular weight of PE (THF GPC) and PDMA/PNIPAm (DMF/LiBr GPC) obtained after hydrolysis.

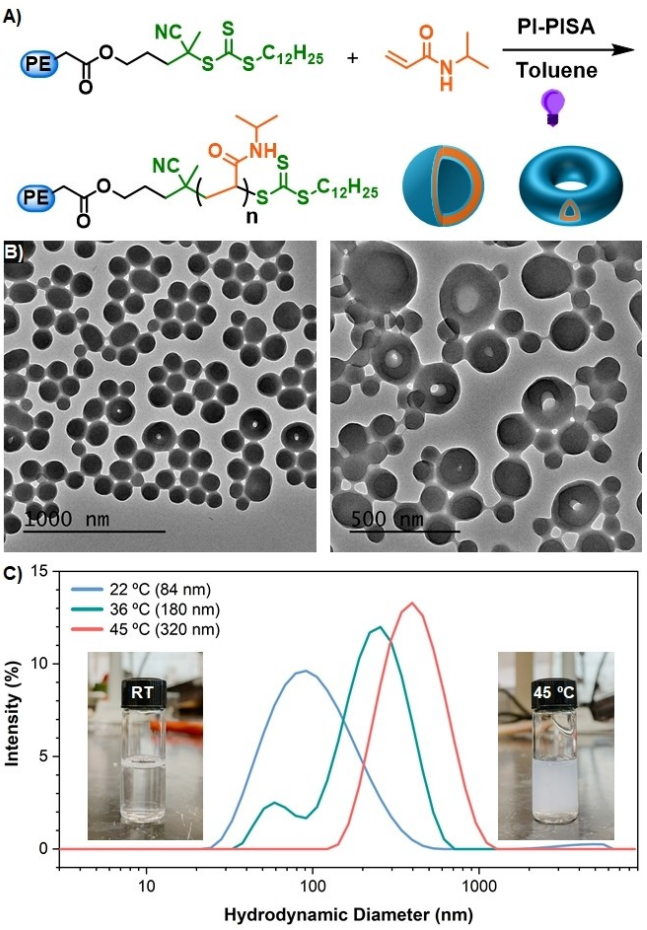

Figure 8. A) PI-RAFT mediated PISA of NIPAM using PE-TTC as a radical source and chain transfer agent. B) Representative TEM image of nanostructures obtained from PISA process. C) DLS size distributions depicted the change in hydrodynamic volume of PE-*b*-PNIPAm diblock copolymer when dispersed in water (0.5 w%).

14500, $Đ = 1.01$; Table 3, Entry 3) as the macroRAFT agent with methyl acrylate (MA), a less challenging monomer. GPC analysis of the crude material obtained after 4 hours of polymerization under UV light showed a new peak appearing at the high molecular weight region in addition to a minor shoulder peak whose retention time was similar to PE-TTC precursor. Nevertheless, the shoulder peak can be easily removed via precipitation/centrifugation using hexane,[8a] affording a well-defined PE-*b*-PMA with $M_n = 35300$, and $Đ = 1.12$ (Figure S42) whose blocky structure was confirmed by the DOSY experiment (Figure S48).

Conclusion

End-functionalized polyolefins serve as an opportunity to join coordination-insertion and other controlled polymerization techniques, which significantly facilitates the development of next-generation materials. In summary, we have developed a strategy that is situated at the interface of pre-functionalized olefin polymerization catalyst development and post-polymerization modification, called the PACE process. The presented approach involves a pentafluorophenyl ester functionalized Pd^{II} diimine catalyst that is used to polymerize ethylene and α-olefins in a living fashion, affording polyolefin precursors bearing the corresponding active ester moiety that can be easily transformed to tailorable functional groups. Additionally, the ability to polymerize long-chain α-olefins in a controlled manner allows crystallinity tuning of the polyolefin segment. This technique not only bypasses the drawbacks such as harsh reaction conditions, as well as the non-uniformity of PE blocks caused by different structural mixtures and molecular weights but also opens the door to a variety of available controlled polymerization methods. These advantages were explored through the preparation of polyolefins bearing hydroxy-, TEMPO•, or trithiocarbonate functional groups, which allow living/controlled polymerization of cyclic esters, styrenic, vinylic, acrylamide, and acrylate monomers via ROP or RDRP. Furthermore, the combination of living polymerization techniques offers fine-tuning options for different polymeric architectures (linear AB, ABC, "star-like" AB_2), molecular weights, and compositions, which correlate directly to the chemical and physical properties of the block copolymers.

Acknowledgements

The authors thank the Robert A. Welch Foundation for the generous support of this research (#H-E-0041 and # E-2066-202110327) through the Center of Excellence in Polymer Chemistry. We gratefully acknowledge the National Science Foundation for support of this work (CHE-2108576 and partially CHE-1808664 (H.D.; E.K. and E.H.); CHE-2108901 (K.M.)). We are grateful to Dr. Xiqu Wang for collecting diffraction data and solving the X-ray structures.

Conflict of Interest

The authors declare no conflict of interest.

Data Availability Statement

Research data are not shared.

Keywords: Block Copolymers · Functionalization · Living Polymerization · Polyolefins · Self Assembly

[1] a) A. Keyes, H. E. Basbug Alhan, E. Ordonez, U. Ha, D. B. Beezer, H. Dau, Y.-S. Liu, E. Tsogtgerel, G. R. Jones, E. Harth, *Angew. Chem. Int. Ed.* **2019**, *58*, 12370–12391; *Angew. Chem.* **2019**, *131*, 12498–12520; b) N. M. G. Franssen, J. N. H. Reek, B. de Bruin, *Chem. Soc. Rev.* **2013**, *42*, 5809–5832.
[2] T. C. Chung, *Prog. Polym. Sci.* **2002**, *27*, 39–85.
[3] a) D. Hustad Phillip, *Science* **2009**, *325*, 704–707; b) P. D. Goring, C. Morton, P. Scott, *Dalton Trans.* **2019**, *48*, 3521–

3530; c) Y. Wang, M. A. Hillmyer, *J. Polym. Sci. Part A* **2001**, *39*, 2755–2766.
[4] a) L. Guo, S. Dai, X. Sui, C. Chen, *ACS Catal.* **2016**, *6*, 428–441; b) L. K. Johnson, C. M. Killian, M. Brookhart, *J. Am. Chem. Soc.* **1995**, *117*, 6414–6415.
[5] a) D. J. Walsh, E. Su, D. Guironnet, *Chem. Sci.* **2018**, *9*, 4703–4707; b) C. J. Kay, P. D. Goring, C. A. Burnett, B. Hornby, K. Lewtas, S. Morris, C. Morton, T. McNally, G. W. Theaker, C. Waterson, P. M. Wright, P. Scott, *J. Am. Chem. Soc.* **2018**, *140*, 13921–13934.
[6] S. M. Stadler, I. Göttker-Schnetmann, A. S. Fuchs, S. R. R. Fischer, S. Mecking, *Macromolecules* **2020**, *53*, 2362–2368.
[7] A. Keyes, H. Dau, K. Matyjaszewski, E. Harth, *Angew. Chem. Int. Ed.* **2022**, *61*, e202112742; *Angew. Chem.* **2022**, *134*, e202112742.
[8] a) H. Dau, A. Keyes, H. E. Basbug Alhan, E. Ordonez, E. Tsogtgerel, A. P. Gies, E. Auyeung, Z. Zhou, A. Maity, A. Das, D. C. Powers, D. B. Beezer, E. Harth, *J. Am. Chem. Soc.* **2020**, *142*, 21469–21483; b) A. Keyes, H. E. Basbug Alhan, U. Ha, Y.-S. Liu, S. K. Smith, T. S. Teets, D. B. Beezer, E. Harth, *Macromolecules* **2018**, *51*, 7224–7232; c) A. Keyes, H. Dau, H. E. Basbug Alhan, U. Ha, E. Ordonez, G. R. Jones, Y.-S. Liu, E. Tsogtgerel, B. Loftin, Z. Wen, J. I. Wu, D. B. Beezer, E. Harth, *Polym. Chem.* **2019**, *10*, 3040–3047.
[9] K. Zhang, Z. Ye, R. Subramanian, *Macromolecules* **2008**, *41*, 640–649.
[10] L. K. Johnson, S. Mecking, M. Brookhart, *J. Am. Chem. Soc.* **1996**, *118*, 267–268.
[11] S. Mecking, L. K. Johnson, L. Wang, M. Brookhart, *J. Am. Chem. Soc.* **1998**, *120*, 888–899.
[12] Deposition Numbers 2173126 contain the supplementary crystallographic data for this paper. These data are provided free of charge by the joint Cambridge Crystallographic Data Centre and Fachinformationszentrum Karlsruhe Access Structures service.
[13] a) S. R. Samanta, R. Cai, V. Percec, *Polym. Chem.* **2015**, *6*, 3259–3270; b) M. Eberhardt, R. Mruk, R. Zentel, P. Théato, *Eur. Polym. J.* **2005**, *41*, 1569–1575; c) A. Das, P. Theato, *Macromolecules* **2015**, *48*, 8695–8707.
[14] A. C. Gottfried, M. Brookhart, *Macromolecules* **2001**, *34*, 1140–1142.
[15] D. J. Tempel, L. K. Johnson, R. L. Huff, P. S. White, M. Brookhart, *J. Am. Chem. Soc.* **2000**, *122*, 6686–6700.
[16] A. C. Gottfried, M. Brookhart, *Macromolecules* **2003**, *36*, 3085–3100.
[17] a) C. M. Killian, D. J. Tempel, L. K. Johnson, M. Brookhart, *J. Am. Chem. Soc.* **1996**, *118*, 11664–11665; b) G. J. Domski, J. M. Rose, G. W. Coates, A. D. Bolig, M. Brookhart, *Prog. Polym. Sci.* **2007**, *32*, 30–92.
[18] E. F. McCord, S. J. McLain, L. T. J. Nelson, S. D. Ittel, D. Tempel, C. M. Killian, L. K. Johnson, M. Brookhart, *Macromolecules* **2007**, *40*, 410–420.
[19] D. Yang, C. Feng, J. Hu, *Polym. Chem.* **2013**, *4*, 2384–2394.
[20] K. Makiguchi, T. Satoh, T. Kakuchi, *Macromolecules* **2011**, *44*, 1999–2005.
[21] M. Kavala, R. Boča, L. Dlháň, V. Brezová, M. Breza, J. Kožíšek, M. Fronc, P. Herich, L. Švorc, P. Szolcsányi, *J. Org. Chem.* **2013**, *78*, 6558–6569.
[22] M. K. Georges, R. P. N. Veregin, P. M. Kazmaier, G. K. Hamer, *Macromolecules* **1993**, *26*, 2987–2988.
[23] a) G. Moad, E. Rizzardo in *Nitroxide Mediated Polymerization: From Fundamentals to Applications in Materials Science*, The Royal Society of Chemistry, London, **2016**, pp. 1–44; b) H. Fischer, *J. Polym. Sci. Part A* **1999**, *37*, 1885–1901.
[24] M. K. Georges, R. P. N. Veregin, P. M. Kazmaier, G. K. Hamer, M. Saban, *Macromolecules* **1994**, *27*, 7228–7229.
[25] H. Willcock, R. K. O'Reilly, *Polym. Chem.* **2010**, *1*, 149–157.
[26] N. D. Hann, *J. Polym. Sci. Polym. Chem. Ed.* **1977**, *15*, 1331–1339.
[27] a) N. J. W. Penfold, J. Yeow, C. Boyer, S. P. Armes, *ACS Macro Lett.* **2019**, *8*, 1029–1054; b) F. D'Agosto, J. Rieger, M. Lansalot, *Angew. Chem. Int. Ed.* **2020**, *59*, 8368–8392; *Angew. Chem.* **2020**, *132*, 8444–8470; c) S. L. Canning, G. N. Smith, S. P. Armes, *Macromolecules* **2016**, *49*, 1985–2001.
[28] a) H. Wang, Q. Li, J. Dai, F. Du, H. Zheng, R. Bai, *Macromolecules* **2013**, *46*, 2576–2582; b) J. F. Quinn, L. Barner, C. Barner-Kowollik, E. Rizzardo, T. P. Davis, *Macromolecules* **2002**, *35*, 7620–7627.
[29] a) A. J. Convertine, B. S. Lokitz, Y. Vasileva, L. J. Myrick, C. W. Scales, A. B. Lowe, C. L. McCormick, *Macromolecules* **2006**, *39*, 1724–1730; b) J. Adelsberger, A. Kulkarni, A. Jain, W. Wang, A. M. Bivigou-Koumba, P. Busch, V. Pipich, O. Holderer, T. Hellweg, A. Laschewsky, P. Müller-Buschbaum, C. M. Papadakis, *Macromolecules* **2010**, *43*, 2490–2501.

Manuscript received: April 22, 2022
Accepted manuscript online: May 19, 2022
Version of record online: June 2, 2022